

Supplementary information

CsdA-LaeB hub governs *Aspergillus fumigatus* virulence via FqC biosynthesis

Zili Song^{1,2,8}, Hongjiao Zhang^{1,8}, Leixin Ye¹, Yuxin Lei¹, Linqi Wang¹, Xiao Liu¹, Nayanna M. Mercado Soto³, Nancy P. Keller³, Berl R. Oakley⁴, Can Zhao^{5,6}, Michael Bromley⁵, Hongwei Liu¹, Lei Cai¹, Koon Ho Wong⁷, Wen-Bing Yin^{1,2 *}

¹ State Key Laboratory of Microbial Diversity and Innovative Utilization, Institute of Microbiology, Chinese Academy of Sciences; Beijing, 100101, PR, China.

² Medical School, University of Chinese Academy of Sciences; Beijing, 100049, PR, China.

³ Department of Medical Microbiology and Immunology, University of Wisconsin-Madison; Madison, 53706, WI, USA.

⁴ Department of Molecular Biosciences, University of Kansas; Lawrence, 66045, KS, USA.

⁵ Manchester Fungal Infection Group, Division of Infection, Immunity and Respiratory Medicine, University of Manchester; Manchester, M13 9NT, United Kingdom.

⁶ Department of Life Sciences, Manchester Metropolitan University; Manchester, M1 5GD, United Kingdom.

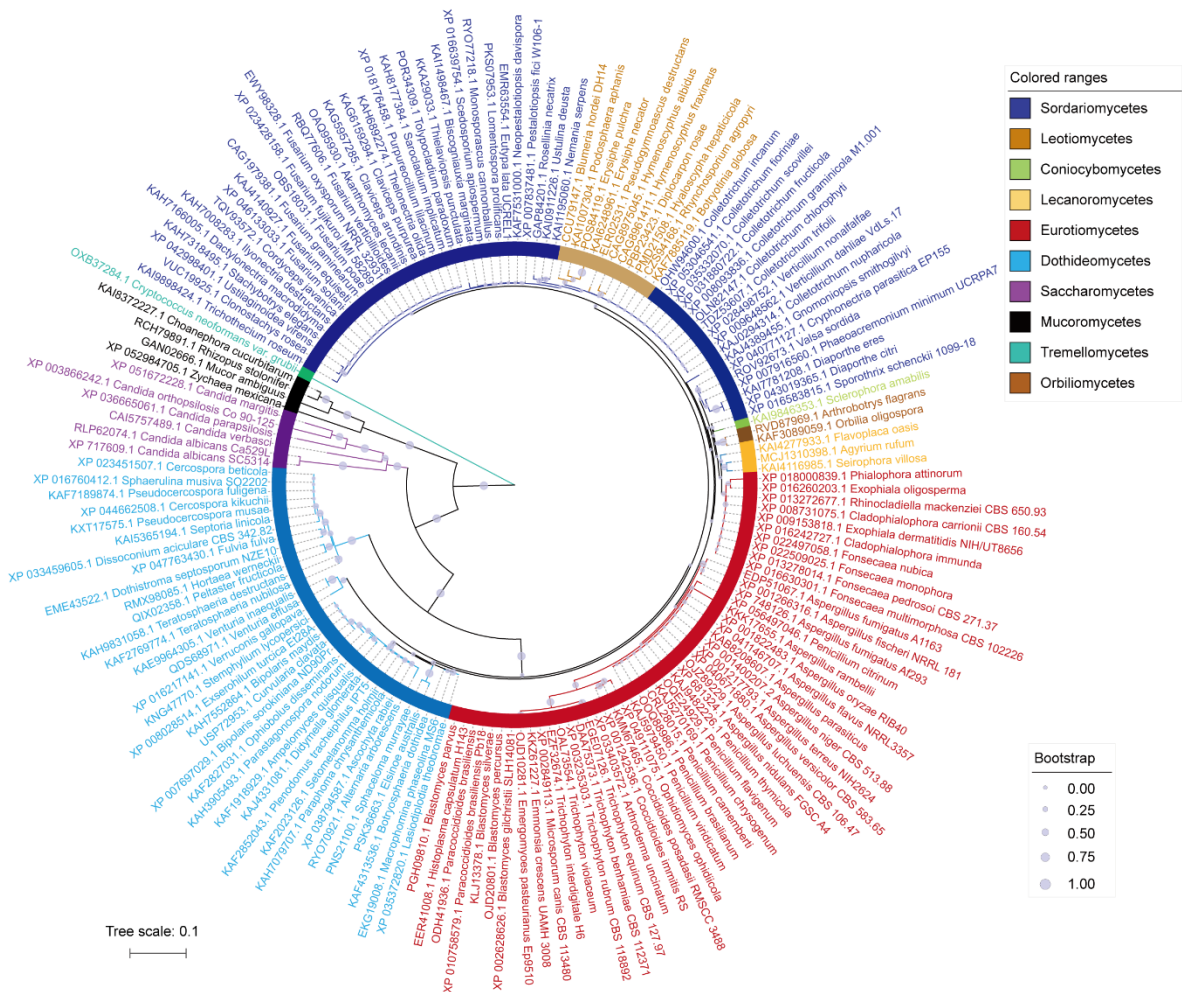
⁷ MoE Frontiers Science Center for Precision Oncology, University of Macau; Macau, SAR, China.

⁸ These authors contributed equally: Zili Song, Hongjiao Zhang

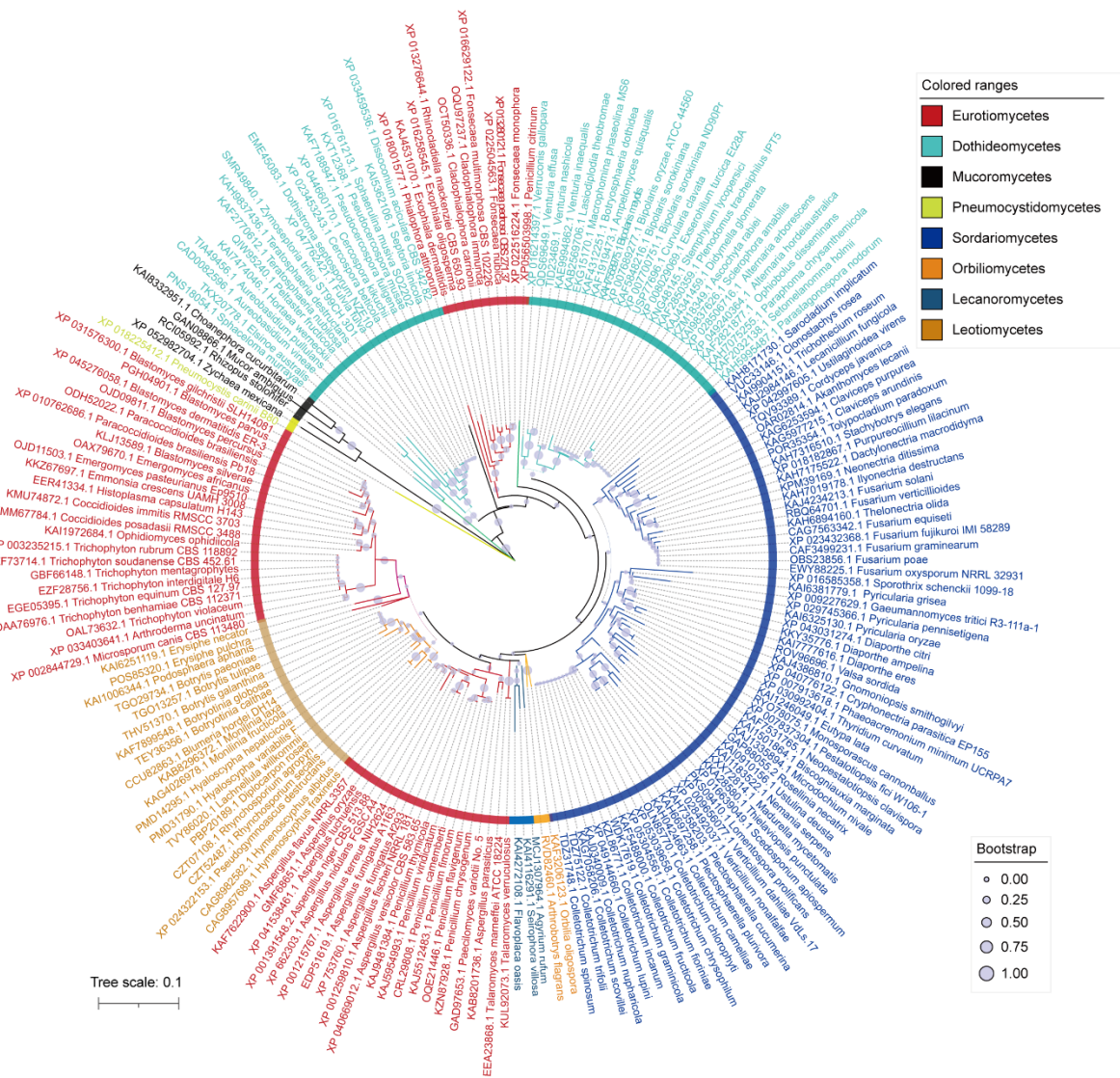
***Corresponding author:** Prof. Dr. Wen-Bing Yin, **Email:** yinwb@im.ac.cn

ORCID: 0000-0002-9184-3198

22 **Supplementary Figure 1**

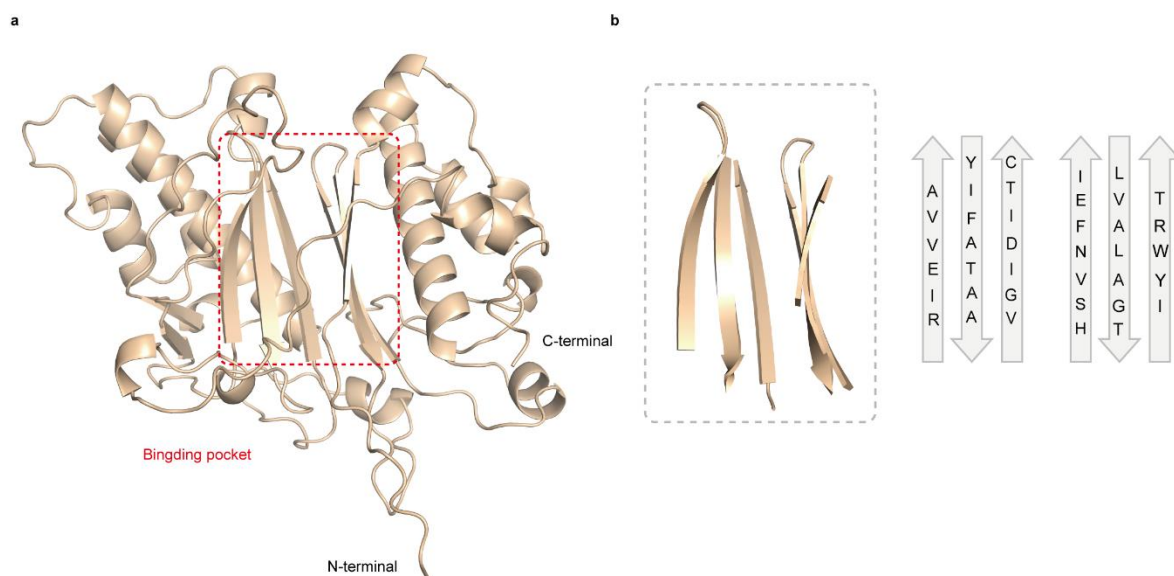


23
24 **Supplementary Fig. 1 Phylogenetic analysis of CsdA in pathogenic fungi.** Phylogenetic tree of the
25 RNA binding protein CsdA in pathogenic fungi. Different colored circles represent taxonomic units of
26 class level. A basidiomycete fungus (*Cryptococcus neoformans* var. *grubii*) was considered as the
27 outgroup. The homologues had more than 30% identity and more than 70% coverage.
28



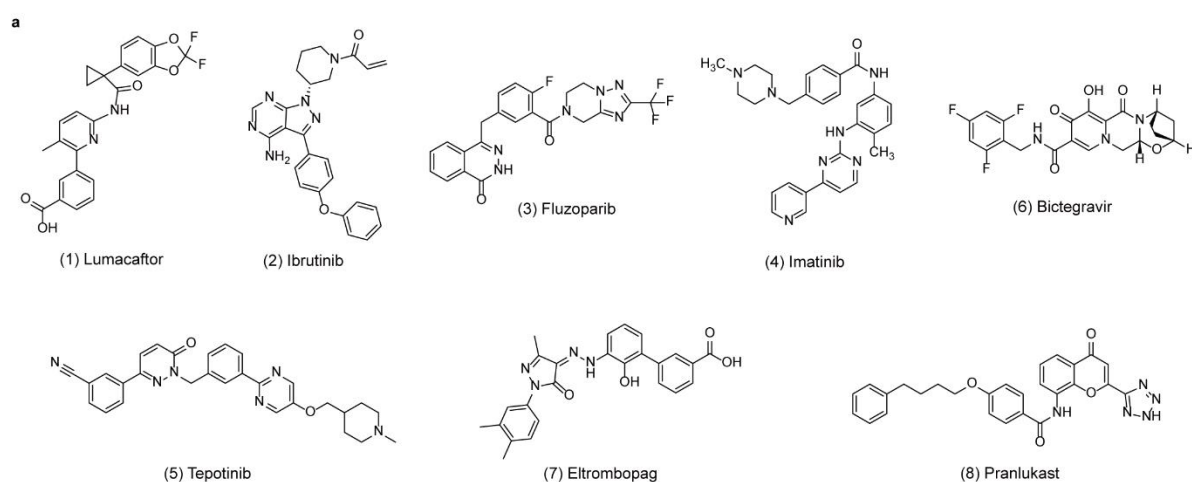
Supplementary Fig. 2 Phylogenetic tree of secondary metabolism global regulator LaeB in pathogenic fungi. Different colored circles represent taxonomic units at the class level. Mucoromycetes fungi were considered as the outgroups. The homologues had more than 40% identity and more than 30% coverage.

Supplemental Figure 3



Supplementary Fig. 3 Binding pocket and amino acid residues in PptA protein. **a**, The predicted three-dimensional structure of PptA protein obtained by AlphaFold2. *N*-terminal, the starting site for protein synthesis. *C*-terminal, the termination site of protein synthesis. **b**, Three-dimensional structure of PptA protein binding pocket. Binding pocket contains six antiparallel β -sheets.

Supplemental Figure 4



b

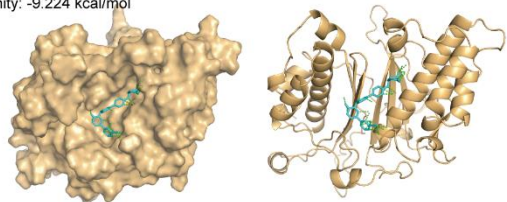
FDA drugs	Clinical trial	Biological activity
(1) Lumacaftor	Cystic Fibrosis, Phase 1, June 2013 Long QT Syndrome, Phase 2, June 15, 2021 Cystic Fibrosis Advanced Lung Disease, Phase 3, March 2015	CFTR modulator
(2) Ibrutinib	Leukemia, Phase 2, February 27, 2012 Chronic Lymphocytic Leukemia, Phase 1, March 9, 2018 Small Lymphocytic Leukemia (SLL) Chronic Lymphocytic Leukemia (CLL), Phase 2, July 31, 2020	Irreversible Btk inhibitor
(3) Fluzoparib	Advanced solid tumor, Phase 1, September 7, 2019 NSCLC Non-small Cell Lung Cancer, Phase 2, July 2023 Ovarian Cancer, Phase 2, December 24, 2021	An orally active PARP1 inhibitor, superior antitumor activity
(4) Imatinib	Gastrointestinal Stromal Tumors, Phase 1, December 1, 2021 Leukemia, Phase 2, April 2001 Kidney Cancer, Phase 2, January 2006	An orally bioavailable tyrosine kinases inhibitor
(5) Tepotinib	FDA approves tepotinib for metastatic non-small cell lung cancer, February 15, 2024	An orally active and highly selective, reversible, ATP-competitive c-Met inhibitor
(6) Bictegravir	HIV-1 Infection, Phase 1, October 24, 2014	A potent inhibitor of HIV-1 integrase
(7) Eltrombopag	Myelodysplastic Syndrome (MDS) Thrombocytopenia, Phase 1, April 6, 2011 Hepatitis C, Phase 1, January 19, 2009	An orally active thrombopoietin receptor nonpeptide agonist
(8) Pranlukast	Chronic Sinusitis, Phase 3, December 2006 Rhinitis, Allergic, Season, Phase 3, November 2004	A highly potent, selective and competitive antagonist of peptide leukotrienes

Supplementary Fig. 4 Structure and clinical trial information of the top 8 drugs with high affinity to PptA. a, Structures of top 8 FDA-approved drug with high affinity for PptA. **b,** Clinical trial information for the top 8 FDA-approved drugs.

49 **Supplemental Figure 5**

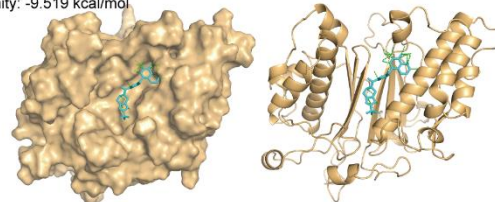
(1) Tepotinib

Affinity: -9.224 kcal/mol



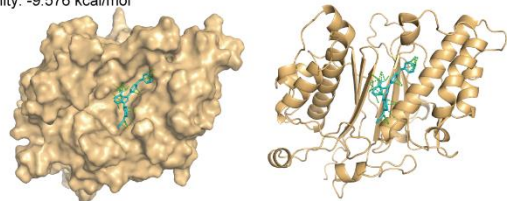
(5) Fluzoparib

Affinity: -9.519 kcal/mol



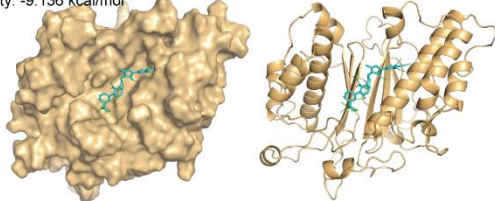
(2) Ibrutinib

Affinity: -9.576 kcal/mol



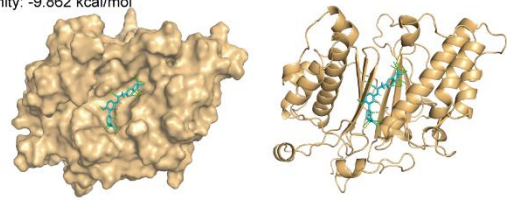
(6) Eltrombopag

Affinity: -9.136 kcal/mol



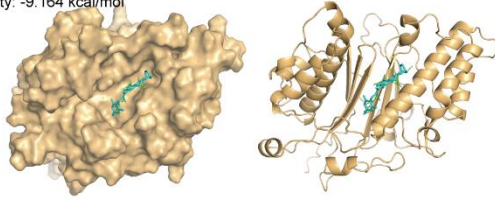
(3) Lumacaftor

Affinity: -9.862 kcal/mol



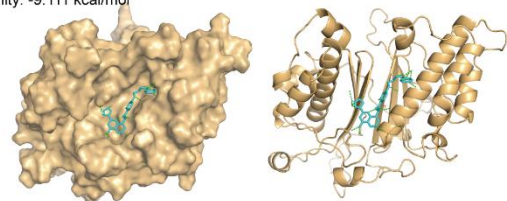
(7) Bictegravir

Affinity: -9.164 kcal/mol



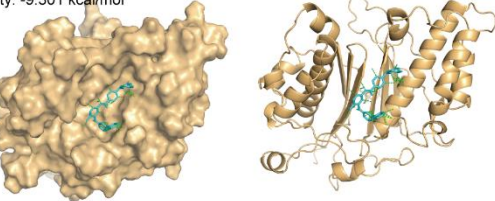
(4) Pranlukast

Affinity: -9.111 kcal/mol



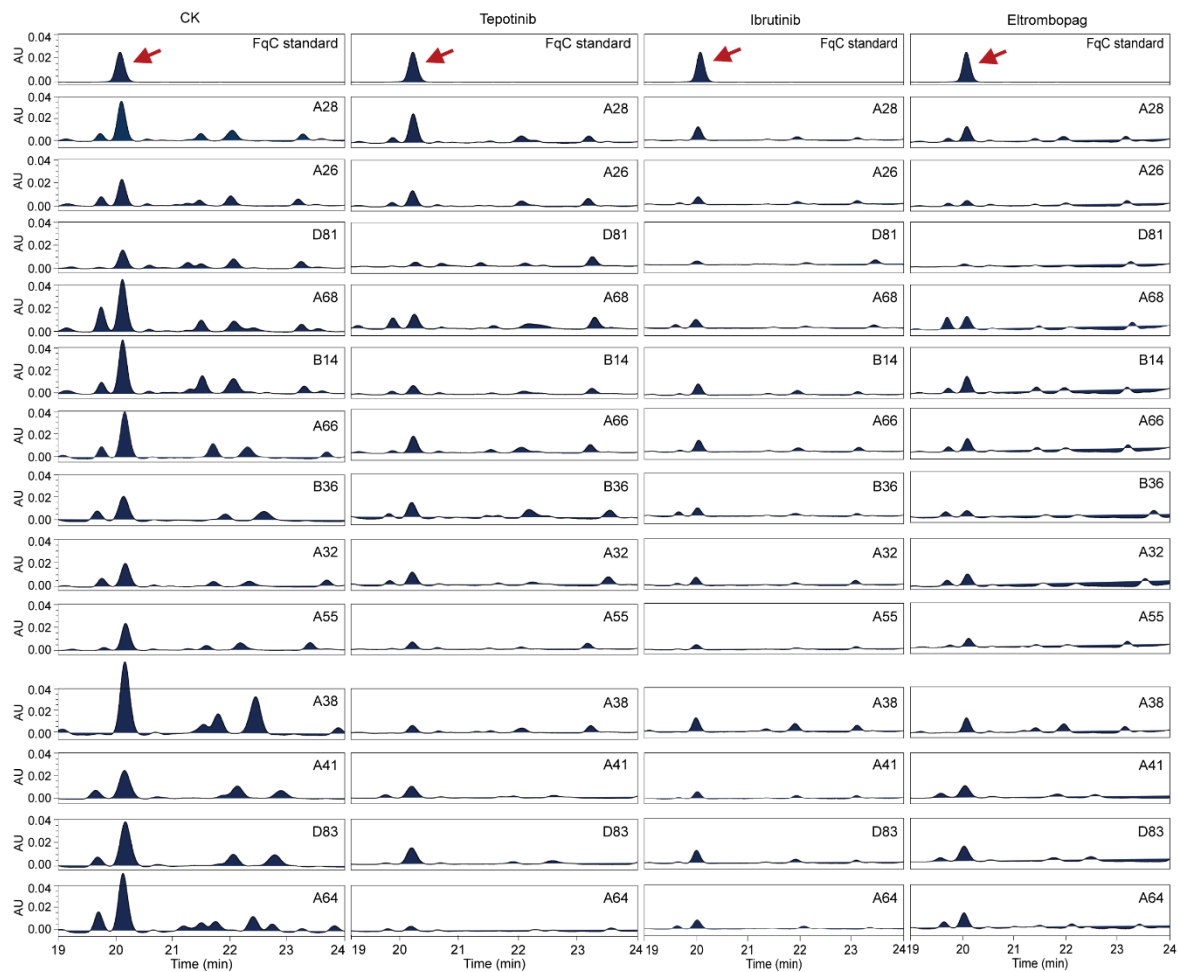
(8) Imatinib

Affinity: -9.301 kcal/mol

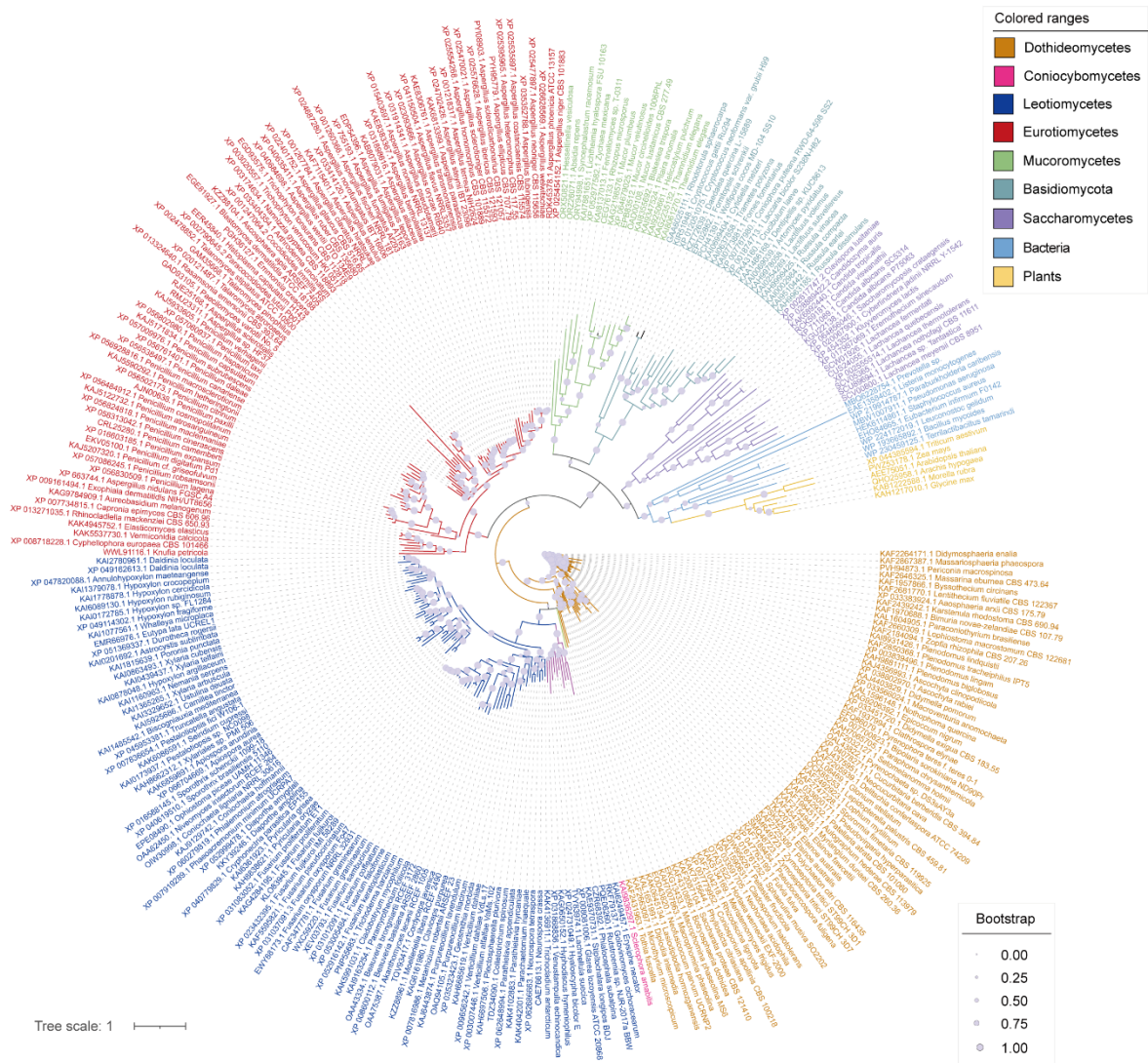


Supplementary Fig. 5 Interaction models of the top 8 FDA-approved drugs with high affinity to PptA. The structures of protein-ligand interaction were visualized by PyMOL software.

54 **Supplemental Figure 6**



55
56 **Supplementary Fig. 6 Metabolites analysis of clinical strains treated with 3 drug candidates.** The
57 metabolic profiles of clinical *A. fumigatus* cultured for 4 days treated with 200 μ M tepotinib, ibrutinib
58 or eltrombopag, respectively. The red arrow represents the peak of fumiquinazoline C.
59



Supplementary Fig. 7 Phylogenetic analysis of the Sfp-type PPTases. Different colors represent taxonomic units of different level. Six plant-derived Sfp-type PPTases were considered as the outgroups.

65 **Supplemental Figure 8**

```

A. fumigatus MGS AQNERIPSLTRWYIDTRQLT-----VTNPSLP LLETLPQSDQEA VKRFYHLRDRHMSLASNLLKYLFIHRS CCIPWNKISI
A. flavus MQPPQDESSNCMVRYIDTRDLT-----ATTTSLP LLETLPQSDQESA KR FYHLKDKHMSLASNLLKYLFIHRTCRIPWNQITI
M. circinelloides -----MAKLDLLSFDIKGAFEG-----DKFDRALSWLPKAEHPSVMRFKFDKDRHLALANLLRRHYFSQELQVPWFDFLEF
F. oxysporum -MMSRTQSSPTVIQWVIDTRPLWPSALKTKDLTSAASRALSLTTEEQSSVLRYYHVRDAKLALASALLKRYAISRFCHVPWFQAKT
C. neoformans -----MYNTIHLSAIIKLPSPEPYD-----KETFDRLASLVLEPPGRERLKRFRRLRDDALRSVLARLTVTWYLYTNGLLPPGELPT
C. gattii -----MYNTIHLSAIIKLPSPEPYD-----KETFDKLASLVDSPARERLARFRLPDDALRSVLARLTVTWYLYTNGLLPPGELPT

A. fumigatus SRTDPDPHRRPCFIPS-PALTEATDEPIPIGIEFNVS HQASLVALAGTIIP-QSHGASPNPTTVFANPSPSSVPAPSPVPQVGI DITC
A. flavus SRTDPAPHRRPYFNAAGFIQTAATDKPIPNIEFNVS HQASLVALAGTILPPSSNND SIAPTNVITNPNPTSTPASSIPQVGI DITC
M. circinelloides DR--LPAGKPYLKHFI-----ESLNYDYNTSHEGDWVIFGCTKDM-----KIGVD AVA
F. oxysporum TR--DARTKPYFVLP-----SGDEPLI---FNVS HQAGLAVLLAVHDP-----PKGLAVGV D VVC
C. neoformans FGR-KAKGKPTLSTP-----NLEPRLEFNNTHEGSYILFTTLRSH-----SPLACVGI D IMK
C. gattii FGR-KKGKPTLLIPI-----KLEPRLEFNNTHEGSYILFTTLRSY-----SPLACVGI D IMK

A. fumigatus VDERHARTSSAPSTRDQLAGYVDIFA EYFSSRELDTIKNLGGRFPADAQDGE--AVEYGLRLFYTYWALK EAYI KMTGEALLAPW
A. flavus VNERRN---TPETRQALEEFVGI FSEYFSQRELDTIKSLHG-VPSHIGNDEEDGLVEYGFRLFYTYWALK EAYI KMTGEALLAPW
M. circinelloides IDRPKKI-----SIDAYLKSFPQLTHNEMHLMVDS DNEDIR-----LET FYQLWGCKE SYTKALGLGLSLD-
F. oxysporum PSERRDR-DLSSLEQDGWASFVDIHADVFGAGEVSALKSMNP-VPA AQERDR-----ALRYFYALWCLREAYY KMTGDALLASW
C. neoformans HPNDPFP-----TQEGIS-----DQLTLL EKQSLAMPLSLRDRS-----LRLTKL WSVKEAYTKAIGEGITFG-
C. gattii HPDDPFP-----TQEGIS-----DQLTLL EKRS LAMPLSARDRS-----LRLTKL WSVKEAYTKAIGEGITFG-

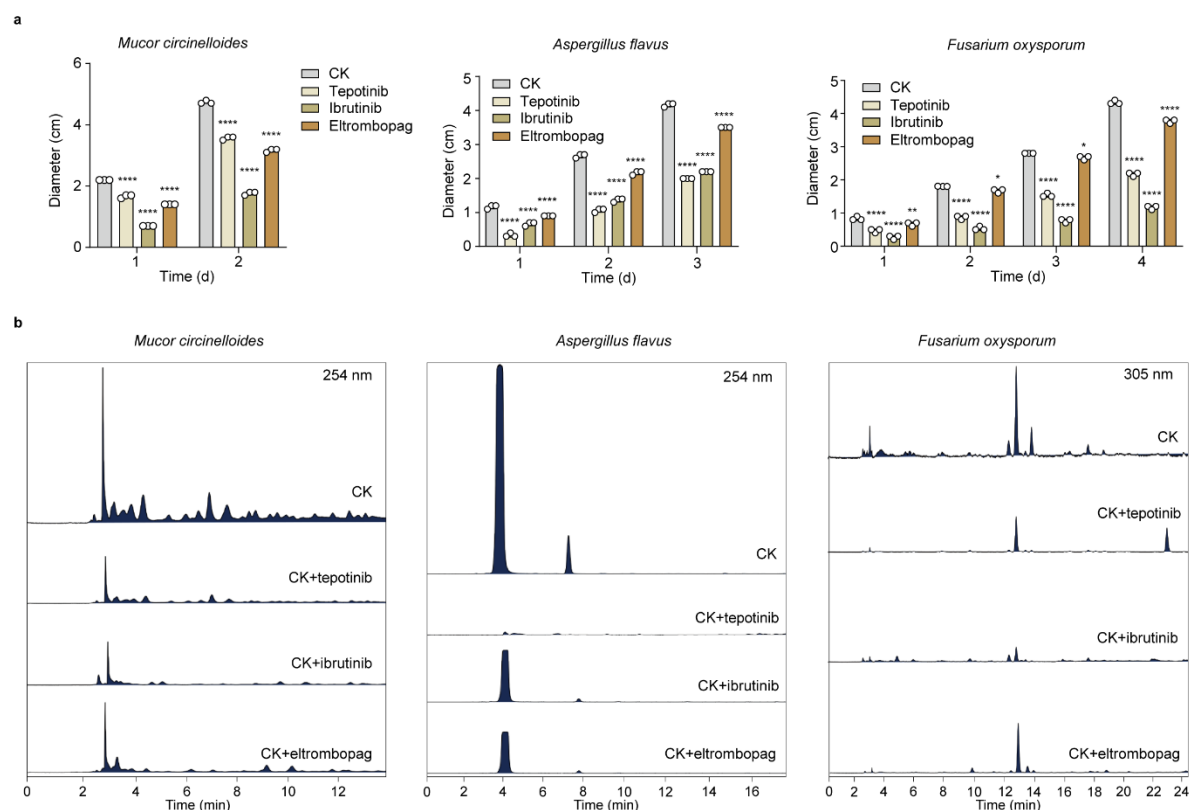
A. fumigatus LRELEF TDVIAPEPAPAGQGSAENWGEPYTGVIWLYGKRVEDVRIEVVAFETGYIFATAARGAGLGAESRPLSRDAGVAVSV D
A. flavus LRELVTNVLAP E PAGR---HLHTWGEPYTGVIWLYGKEVEDVRLLEVAFENDYLIATAARGGGIGWRS---EGDG---AD
M. circinelloides LLKLDFSNVQDTI-----KMKFDGQQLDNWVFFYLDRLD DTTLAVVCCGFIETSQLDSGII EFSR--LTQ
F. oxysporum LKDL E MHNFA PPE-----DMEEAQEVRLRGKKV EGV D VRLMPLLEEYMI STAVRNGDNGERV-----
C. neoformans LERIEVELSASAG-----KVERVKVDGRD V DERGW EWRVGEIGEDYGWA V WVRGSDVEREL-----
C. gattii LERIEVELSAGAG-----KVERVKVDGRD V DERGW EWRVGEIGEDYGWA V WVRGDDYERKL-----

A. fumigatus RWMHMEKIDIDRDIA PCATGVCQCTKK-----
A. flavus PWQRLEKIDIEKDVRPCATGVCQCLK-----
M. circinelloides LLGKRSQMKKDTDIFHQIKLQDI ENNKWMPRS
F. oxysporum ELGEFQSLDMEEVLAFGEKASKS-----
C. neoformans VIDHISWEDFVRPLLVLAE S RLTSNT-----
C. gattii VIDHISWEDFARPLLVLAE S RLTSNT-----

```

66
67 **Supplementary Fig. 8** Conservative analysis of drug binding sites in fungal Sfp-type PPTases.
68 Binding sites D159, W227, E231, and K235 of the three drug candidates were conserved in fungal Sfp-
69 type PPTases, including *A. fumigatus*, *A. flavus*, *Mucor circinelloides*, *Fusarium oxysporum*,
70 *Cryptococcus neoformans*, and *Cryptococcus gattii*.
71

Supplemental Figure 9



Supplementary Fig. 9 Growth and metabolite analysis of other pathogenic fungi treated with 3 drug candidates. a-b, Evaluation of growth (a) and metabolism (b) of filamentous fungi *M. circinelloides*, *A. flavus* and *F. oxysporum*. The metabolic profiles of *M. circinelloides* treated with 200 μ M drugs at 28°C for 3 days. The metabolic profiles of *A. flavus* treated with 200 μ M drugs at 37°C for 4 days. The metabolic profiles of *F. oxysporum* treated with 200 μ M drugs at 28°C for 5 days. All error bars are expressed as \pm SD. Statistical analysis was performed by using Two-way ANOVA (“ns”: not significant. Significant at * $p < 0.05$, ** $p < 0.01$, *** $p < 0.0001$).